TRASC: Tensor-based Radio Spectrum Cartography using Plate Splines and Tensor CP Decomposition

Mohsen Joneidi, Nazanin Rahnavard and Farzam Hejazi

Department of Electrical and Computer Engineering

University of Central Florida, Orlando, FL 32816

Emails: {mohsen.joneidi, nazanin.rahnavard, farzam.hejazi}@ucf.edu

Abstract—The problem of radio spectrum cartography is addressed based on simultaneous tensor decomposition and interpolation of spatial maps. To this aim, a joint problem of CANDECOMP/PARAFAC (CP) decomposition and thin-plate splines is introduced and solved efficiently. Spectrum cartography is known as estimating power spectrum in any arbitrary location and frequency based on a small subset of sensed locations and frequencies. Tensor-based radio spectrum cartography (TRASC) algorithm is proposed to address spectrum cartography which consists of iterative solutions for two subproblems. The tensor decomposition subproblem models the latent temporal and spectral structure of sources, and the interpolation subproblem takes into the account fine spatial details in order to leverage neighborhood information within a certain vicinity. From mathematical point of view, retrieving non-sensed data from incomplete measurements is an ill-posed inverse problem. We utilize an assumption on rank of tensors and an assumption on smoothness of spatial interpolated maps to make the joint problem well-posed. Moreover, the impact of dynamics of the network on the rank of the underlying tensor is studied. The simulation results show applicability of the proposed algorithm in spectrum map estimation in presence of multi-dimensional sensing results over time, frequencies and space. Our experiments indicate that utilizing tensors and spatial interpolation is an effective approach for spectrum cartography.

Index Terms—Cognitive radio networks, dynamic spectrum sensing, radio cartography, and CP tensor decomposition.

I. INTRODUCTION

Spectrum cartography is a promising solution to address today's spectrum deficiency caused by the recent spike in demand for wireless technologies [1–3]. The licensed holders of the spectrum (a.k.a. primary users or PUs) often under-utilize this valuable resource [4]. It is desired to allow unlicensed or secondary users (SUs) to coexist with PUs given that they do not interfere with the licensed users. This necessitates a cognitive radio system to sense the spectrum usage and accordingly adapt its spectrum utilization [5, 6].

The spectrum sensing problem is approached using numerous methods [7]. These methods are ranged from per-bin spectrum sensing [8] to wide-band sensing [9]; non-cooperative sensing [10] to cooperative sensing [11]; centralized [12] to distributed [13]; and directional sensing [14] using phased arrays [15] to omni-directional energy detectors. Our work focuses on cooperative centralized spectrum sensing using a set of simple energy detectors. Cooperative detection of spectrum opportunities requires collecting sensed measurements

This material is based upon work supported by the National Science Foundation under Grant No. CCF-1718195 and ECCS-1810256.

in a fusion center. However, dealing with a large amount of spectrum measurements is not a trivial task. Efficient representation using high-dimensional matrices/tensors is an attractive approach for analysis of sensed measurements. In this way, structured factorization of the received spectrum enables us to capture the underlying spectrum occupancy patterns [16–18]. In the present work, we model the propagated power from the primary transmitters at different locations, time slots, and frequency channels as a multi-dimensional tensor, which is referred to as *the power tensor*.

The radio frequency (RF) cartography problem leads to find the propagating power maps across a network at any frequency channel. This is an ill-posed problem, and therefore it is difficult to infer unique and meaningful interpretation for the estimated propagating power maps. To alleviate this issue, we consider the CANDECOMP/PARAFAC (CP) [19] model for the latent tensor and we impose smoothness constraint for the interpolated spatial maps. The CP model represents a D-dimensional tensor via D factor matrices. Each factor matrix contains a set of bases that spans one way of the tensor. Here, we deal with 3-way tensors, i.e., D = 3. In the proposed framework, the CP factors capture the patterns of the PUs' activities over different dimensions of time, space, and frequency. We propose the tensor-based radio spectrum cartography (TRASC) algorithm to address the joint problem of tensor decomposition and map interpolation. CP [19] and Tucker [20] are two well-known tensor decomposition methods, which can be interpreted as two extensions of matrix singular value decomposition (SVD). The main contributions of the paper are summarized as follows:

- Dynamic spectrum cartography is modeled by a low-rank tensor and the relationship between the imposed rank and the dynamics of network is studied,
- A novel algorithm, referred to as TRASC, is introduced that performs spatially-smooth tensor completion using tensor decomposition and spatial interpolation.
- The applicability of TRASC for spectrum cartography with unknown propagation parameters is demonstrated.

Notations: Throughout this paper, vectors, matrices, and tensors are denoted by bold lowercase, bold uppercase, and bold underlined uppercase letters, respectively. The positive orthant in \mathbb{R}^P is denoted by \mathbb{R}_+^P and it is defined as $\{\boldsymbol{x}|x_p\geq 0, \forall p=1,\cdots,P\}$, in which x_p is the p^{th} element of \boldsymbol{x} . If $\underline{\boldsymbol{T}}\in\mathbb{R}^{P\times F\times T}$ then $(\underline{\boldsymbol{T}})_{:,f,t}$ is a vector of length P, also

known as a mode-1 fiber of T, defined by fixing all the indices but one. Similarly, we have mode-2 and mode-3 fibers. T_1 , T_2 , and T_3 are unfolded matrices whose columns are fibers of the first, second and third mode of T, respectively. The Khatri-Rao product is denoted by ⊙. Moreover, ∘ denotes the outer product, i.e., entries of $\underline{T} = a \circ b \circ c$ are calculated as $t_{pft} = a_p b_f c_t$. The outer product of two non-zero vectors is a rank-1 matrix, similarly the outer product of three non-zero vectors is a rank-1 tensor. The symbol * denotes the elementwise (Hadamard) product. The n-mode product of a tensor, X, with a proper sized transformation matrix U is a tensor and is denoted by $\underline{X} \times_i U$. It transfers each fiber of the i^{th} mode of the tensor to the corresponding fiber in the output tensor. Mathematically, $\underline{Y} = \underline{X} \times_i U \leftrightarrow Y_i = UX_i$ for i = 1, 2, 3, in which X_i and Y_i are unfolded replicas of tensor X and Yw.r.t. different dimensions. $X \ge 0$ indicates that every element in \underline{X} is non-negative.

II. PRELIMINARIES

A. CP Decomposition

Our proposed tensor-based approach is mainly based on the CP decomposition [21], which factorizes a tensor into a sum of rank-one tensors. For example, a three-way tensor $\underline{\boldsymbol{X}} \in \mathbb{R}^{P \times F \times T}$ of rank R can be decomposed as

$$\underline{\boldsymbol{X}} = \sum_{r=1}^{R} \boldsymbol{a}_{r}^{X} \circ \boldsymbol{b}_{r}^{X} \circ \boldsymbol{c}_{r}^{X} = [\![\boldsymbol{A}_{X}, \boldsymbol{B}_{X}, \boldsymbol{C}_{X}]\!], \tag{1}$$

where $a_r^X \in \mathbb{R}^P$, $b_r^X \in \mathbb{R}^F$ and $c_r^X \in \mathbb{R}^T$ are factor vectors of the r^{th} rank-one component. The factor matrices refer to the collection of factor vectors from the rank-one components, i.e., $A_X = [a_1^X \ a_2^X \ \dots \ a_R^X]$ and likewise for B_X and C_X .

The tensor CP rank may be referred to as unconstrained rank because there is no additional constraint on the factors a_r^X , b_r^X and c_r^X . On the other hand, there is the constrained or structured rank in which the factors are restricted to be within a specific set [21]. For example, non-negative-rank and symmetric-rank are obtained by imposing nonnegativity and symmetry constraints on the factors, respectively.

Due to corruption by noise, typical tensors are not low rank and low-rank approximation should be employed in order to extract a set of meaningful components. However, low-rank approximation of tensors is an ill-posed problem. This is because the set of tensors with the rank of at most R is not a closed set and optimization algorithms for finding CP factors result in an infimum solution which is not feasible [22]. There are some efforts for approximating rank with other functions such as nuclear norm¹ [24]. In contrast to the matrix rank minimization, tensor rank minimization cannot be relaxed easily using nuclear norm because the calculation of tensor nuclear norm is an NP-hard problem [24]. Alternating least squares (ALS) is a well-known method for finding the CP factors [25] of a tensor X, in which factors are initialized randomly at the beginning and then updated iteratively.

B. Spline-based Surface Interpolation

Spectrum map of an area contains spatial correlation over neighboring locations. Our proposed framework estimates a set of principal incomplete spectrum maps such that the actual sensed data is a linear combination of them. The principal incomplete maps are estimated using CP decomposition. Interpolation of the principal incomplete maps (spatial CP factors) is the enabling step toward estimating the actual spectrum map for any arbitrary location. Please note that the contribution of each principal map can be estimated using CP decomposition and the same contribution coefficients are applied for reconstructing the full spectrum map using the interpolated principal maps. In the present work, thin plate splines (TPS) is employed for interpolating the spatial incomplete maps [26]. TPS is proposed for modeling climate data originally. However, it is an efficient model for capturing other kinds of spatial dependencies including spectrum cartography [26].

Assume we are given a set of locations (z_n, w_n) and their corresponding value y_n . The problem of surface interpolation can be cast as finding function $f: \mathbb{R}^2 \to \mathbb{R}$ such that $f(z_n, w_n)$ is as close as possible to y_n and at the same time a desirable property is satisfied for function f. Specifically, in TPS a measure for smoothness of f is employed as follows [27],

$$I_f = \int \int \left(\frac{\partial^2 f}{\partial z^2} + 2 \frac{\partial^2 f}{\partial z \partial w} + \frac{\partial^2 f}{\partial w^2} \right) dz dw.$$
 (2)

The coefficient I_f is called the bending energy of f. Function f is modeled by summation of n terms given by

$$f(z,w) = \sum_{i} \lambda_{i} r_{i}^{\alpha} log(r_{i}), \tag{3}$$

where $r_i = \sqrt{(z-z_i)^2 + (w-w_i)^2}$. Equation (3) describes the kernel of interpolation. Parameter α is the path-loss coefficient which is set to 2 for power spectrum propagation in free space. The goal of interpolation is to find function f and it can be expressed mathematically as follows,

$$\underset{f}{\operatorname{argmin}} I_f \text{ s.t. } y_n = f(z_n, w_n).$$

Finding an optimized interpolating function is equivalent to estimating λ_i 's according to (3). Here, for simplicity of notation the minimization is shown w.r.t. function f. In the next section, the thin plate spline interpolation is integrated with the CP decomposition in order to address the spectrum cartography problem under missing sensor measurements.

III. THE TRASC ALGORITHM

This section presents our main contribution. First, the tensor-based problem formulation for spectrum cartography is introduced. The derived formulation is based on partitioning the area to a grid network and modeling the received spectrum at each grid point by a superposition of the propagating power from sources. Then, practical assumptions are elaborated to make the problem tractable and a discussion for rank estimation is exhibited. We suppose the locations of SUs are known and the goal is to find the propagating power and location of

¹Nuclear norm is a well-known function to surrogate rank of matrices [23].

active PUs as the enabling step for reconstructing the power spectrum map at any arbitrary location and frequency. To achieve this, let us consider a set of grid points across the area of interest. Let N denote the number of grid points in the area of interest and G denotes the number of active primary users. The indices of sensors is a subset of $\{1, \cdots, N\}$. The frequency bandwidth is broken into F frequency channels. The received PSD at location/sensor n at time t and frequency channel f can be written as $[11]^2$,

$$y_n(t,f) = \sum_{g=1}^{G} \phi_{ng} x_g(t,f) + z_n(t,f)$$

$$= \boldsymbol{\phi}_n^T \boldsymbol{x}(t,f) + z_n(t,f),$$
(4)

where, $\phi_n = [\phi_{n1} \cdots \phi_{nG}]^T$, in which ϕ_{ng} is the channel gain between the g^{th} active source and the n^{th} sensor. The total number of active sources is indicated by G. The propagation from the g^{th} active source is denoted by $x_g(t,f)$ and the collection for all grid points forms vector $\boldsymbol{x}(t,f) = [x_1(t,f) \cdots x_G(t,f)]^T$. We assume the measurements are available for T time slots and F frequency channels. Collaborative estimation of $\boldsymbol{x}(t,f) \in \mathbb{R}^G$ over each time slot and for each frequency bin requires collecting measurements of all sensors in vector $\boldsymbol{y}(t,f) = [y_1(t,f) \cdots y_N(t,f)]^T \in \mathbb{R}^N$. The following minimization problem has been proposed for estimation of $\boldsymbol{x}(t,f)$ for each time and frequency independently [11]

$$\boldsymbol{x}(t,f) = \underset{\boldsymbol{x}}{\operatorname{argmin}} \|\boldsymbol{y}(t,f) - \boldsymbol{\Phi} \boldsymbol{x}\|_{2}, \tag{5}$$

where the n^{th} row of matrix Φ is ϕ_n^T . The regularized version of (5) using ℓ_1 constraint has previously been employed for collaborative spectrum estimation for a given Φ [11, 28, 29].

Let us represent the collection of $\boldsymbol{x}(t,f)$ and $\boldsymbol{y}(t,f)$ for all frequencies and time slots as tensors $\underline{\boldsymbol{X}} = [x_{gtf}]$ and $\underline{\boldsymbol{Y}} = [y_{ntf}]$, respectively. That is $x_{gft} = x_g(t,f)$ and $y_{nft} = y_n(f,t)$. Tensor $\underline{\boldsymbol{X}} \in \mathbb{R}^{G \times F \times T}$ is referred to as *power tensor* and tensor $\underline{\boldsymbol{Y}} \in \mathbb{R}^{N \times F \times T}$ is referred to as *cartography tensor*. Please note that $\boldsymbol{x}(t,f)$ is a vector in \mathbb{R}^G and $\boldsymbol{y}(t,f)$ is a vector in \mathbb{R}^N . These vectors point to the mode-1 fibers of $\underline{\boldsymbol{X}}$ and $\underline{\boldsymbol{Y}}$, respectively. We aim to estimate the propagation power from each active source using the accessible measurements in \boldsymbol{Y} . Mathematically speaking, we have:

$$\underline{Y} = \underline{X} \times_1 \Phi + \underline{Z}. \tag{6}$$

Each entry of matrix $\Phi \in \mathbb{R}^{N \times G}$ represents the channel gain between the n^{th} grid point and the g^{th} source [11]. Our goal is to estimate the power tensor, \underline{X} , which is characterized by its CP factors. Due to narrow band communication, and the temporal correlation of power propagation at a transmitter, tensor \underline{X} is highly structured and can be modeled by a low-rank tensor using the CP decomposition as stated in (1). Each rank-1 tensor, i.e., $a_r^X \circ b_r^X \circ c_r^X$, represents a principle pattern of the spectrum propagation. Matrix Φ consists of G number of vectorized maps in which each map is a reshaped version of

a column of Φ . Let define tensor $\underline{\Gamma} \in \mathbb{R}^{\sqrt{N} \times \sqrt{N} \times G}$ such that the g^{th} slice of $\underline{\Gamma}$ is the reshaped version of the g^{th} column of Φ . Without loss of generality we assume that N is a perfect square number and the area of interest consists of $\sqrt{N} \times \sqrt{N}$ grid points. Moreover, let us define multiplication operator $\langle \cdot, \cdot \rangle$ such that

$$\langle \underline{X}, \underline{\Gamma} \rangle = \underline{X} \times_1 \Phi.$$
 (7)

It is interesting to mention that the CP factors of tensor \underline{Y} in the presence of no noise, i.e., $\underline{Z} = 0$, can be stated as follows in terms of CP factors of tensor X:

$$a_r^Y = \Phi a_r^X, b_r^Y = a_r^X, c_r^Y = c_r^X.$$
 (8)

Tensor $\underline{\Gamma}$, which is a reshaped version of matrix Φ , plays a key role in our architecture. Each slice of this tensor contains an incomplete power propagation pattern from a source. Interpolating these patterns alongside with tensor \underline{X} results in a completed cartography tensor, \underline{Y} . Solving the following problem provides us with two outcomes: (i) the CP factors of the power tensor and (ii) principle propagation maps and their interpolation functions.

Since sensors are distributed in a small subset of $\{1, \dots, N\}$, we need to reduce the problem to only the known information. Function Ω reduces the problem into only the sensed locations. Function f_q interpolates the incomplete power spectrum map corresponding to the g^{th} slice of $\underline{\Gamma}$. The bending energy of $f_g(z, w)$ is denoted by I_g which is defined in (2) and variable α controls smoothness of the interpolation function. Each slice of tensor $\underline{\Gamma}$ is a 2D incomplete surface since the sensed tensor \underline{Y} is incomplete. Interpolation of all slices of $\underline{\Gamma}$ results in completion of \underline{Y} . Please note that each slice of Γ exploits a separate interpolating function. This problem can be regarded as a combination of CP decomposition and 2D surface interpolation. Here, we assume that sources are distinguished based on their spatial distance and their spectral signature over time. For example, if the spectral pattern of propagating power from a location is changed after a certain time, two distinguished sources are accounted.

Parameters G and R depend on the actual number of active users. However, the actual number of active users is unknown in a realistic network. Therefore, a large enough estimation can be substituted. In order to make the model more parsimonious, we assume R=G. The problem can then be simplified to the following form by elimination of parameter G and the auxiliary variable X as

$$\underset{\boldsymbol{\phi}_r, \boldsymbol{b}_r, \boldsymbol{c}_r, f_r}{\operatorname{argmin}} \|\Omega(\underline{\boldsymbol{Y}} - \sum_{r=1}^R \boldsymbol{\phi}_r \circ \boldsymbol{b}_r \circ \boldsymbol{c}_r)\|_F^2 + \alpha \sum_r I_r$$
subject to:
$$f_r(z_i, w_i) = \boldsymbol{\Gamma}_r(z_i, w_i) \ \forall \ i \in \mathbb{O}.$$

²This form requires a set of mild conditions which is out of scope our present work and studied in [11]

In this problem, ϕ_r is the vectorized replica of the r^{th} principle spectrum map and it can be interpreted as a CP factor of tensor Y w.r.t. the spatial dimension. In other words, the first CP factor is regularized to have the minimum bending energy in order to have a smooth map over interpolated locations. Since \underline{Y} is an incomplete tensor w.r.t. non-sensed locations, there are enough information to estimate a subset of entries of ϕ_r . However, a spatial interpolation can reveal us a completed principle map. Each principle map is interpolated using a function which is regularized to have a smooth behavior. This regularization is inspired by prior work in the literature of interpolation as discussed in Sec. II-B. The interpolator function is constrained to be equal to the principle maps at the observed locations indexed in set \mathbb{O} . The coordinate of observed locations are shown by (z_i, w_i) . Low-rank assumption for the cartography tensor is helpful for making the problem identifiable. However, fine local details of the spectrum maps are lost in the found low-rank structure. Two dimensional interpolation is employed in order to keep details in the sensed data and to infuse these details for interpolation of non-sensed locations. Surface interpolation helps CP factors to obtain spatial smooth factors. ALS is the practical approach for solving the proposed problem in which each iteration corresponds to a least squares problem with missing entries (will be explained in Section III-B). Interpolating b_r and c_r results in increasing both spectral and temporal resolution.

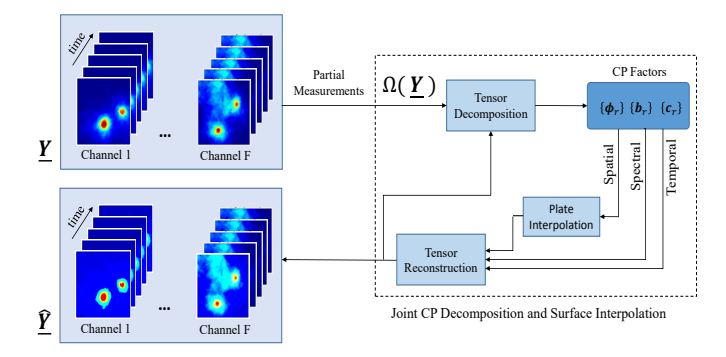


Fig. 1: Framework of the proposed joint tensor decomposition and surface interpolation. This scheme only shows a big picture of the proposed work. Practically, CP decomposition is implemented iteratively. In the proposed algorithm, interpolation is performed alongside iterations of CP decomposition. In other words, we solve a joint problem of decomposition and interpolation.

A. Least Square Solution with Missing Entries

Our main proposed algorithm requires solving a general least square problem with missing entries along iterations. Let us formalize this problem as follows for a given matrix Y, a given matrix X, and known entries organized in a binary matrix denoted by M,

$$\hat{A} = \underset{A}{\operatorname{argmin}} \| M * (Y - XA) \|_F^2$$
 (11)

The solution of this problem w.r.t. A given Y, X, and the mask is straightforward which is indicated in Alg. 1 referred to as missing entries least squares (MELS). Please note that MELS solves a basic optimization problem and our main

proposed algorithm is built upon it iteratively. In MELS, each column of A can be computed independently. Alg. 1 is a

Algorithm 1 Missing Entries Least Squares (MELS)

```
Require: \boldsymbol{Y} \in \mathbb{R}^{N \times F}, \boldsymbol{X} \in \mathbb{R}^{N \times R}, and the available entries set, \Omega.

Output: \boldsymbol{A} \in \mathbb{R}^{R \times F}.

1: Compute \boldsymbol{M} \in \mathbb{R}^{N \times F} based on Set \Omega
FOR f = 1, \dots, F

2: \boldsymbol{D} = \operatorname{diag}(\boldsymbol{M}(:, f))

3: \boldsymbol{W} = \boldsymbol{X}^T \boldsymbol{D} \boldsymbol{X}

4: \boldsymbol{A}(:, f) = \boldsymbol{W}^{-1} \boldsymbol{X}^T \boldsymbol{D} \boldsymbol{Y}(:, f)
END FOR
```

simple solution for (11) and plays a key role in our main algorithm. The solution of (11) is referred as $MELS(Y, X, \Omega)$.

B. Implementation of TRASC for Power Map Reconstruction

Here a practical algorithm for solving (10) is proposed. The sensed incomplete tensor is decomposed into a set of CP factors considering the known entries. Then, the spectral and temporal factors are kept and spatial factors are interpolated in each iteration of tensor decomposition. The power spectrum at any arbitrary location and in each frequency can be inferred via tensor reconstruction of CP factors. Alg. 2 presents the steps of the TRASC algorithm that is a *joint tensor decomposition* and 2D interpolation for spectrum cartography. Spectral and temporal CP factors, i.e., matrices B and C, are initialized by a plain CP decomposition on \underline{Y}_{Ω} where unknown entries are set to 0. The initial value for spatial factors is estimated using the MELS algorithm. In Alg. 2, TPS(.) refers to thin-plate splines interpolation method, introduced in Sec. II-B.

Algorithm 2 Tensor-based Radio Spectrum Cartography

```
Require: \underline{\boldsymbol{Y}}_{\Omega}, R, \Omega, \alpha and N.
Output: \underline{\underline{Y}}
1: Initialize B and C by CP factors of \underline{Y}_{O}
2: \Phi \leftarrow \text{MELS}(\mathbf{Y}_1^T, \dot{\mathbf{B}} \odot \mathbf{C}, \Omega)
      While (The stopping criterion is not met)
3:
                  \boldsymbol{B} \leftarrow \text{MELS}(\boldsymbol{Y}_2^T, \boldsymbol{C} \odot \boldsymbol{\Phi}, \Omega)
                 C \leftarrow \text{MELS}(\mathbf{Y}_3^T, \mathbf{B} \odot \mathbf{\Phi}, \Omega)
4:
5:
                  FOR t = 1 \dots T
                         F = B \operatorname{diag}(C_t)
6:
                         m{A}_{\Omega}^t = (m{F}^{\dagger} m{Y}_{\Omega}^t)^T
7:
8:
                        FOR r=1 \dots R
9:
                                 \Gamma_r = \text{TPS}(\text{reshape}(\boldsymbol{a}_{\Omega}^t, [\sqrt{N}, \sqrt{N}]), \Omega, \alpha)
                                   \phi_r = \operatorname{vec}(\Gamma_r)
10:
                          END FOR
                         Y^t = \Phi F^T
11:
                  END FOR
      END While
```

In Alg. 2, $\mathbf{Y}^t = \underline{\mathbf{Y}}(:,:,t)$ is a slice of tensor $\underline{\mathbf{Y}}$ corresponding to time slot t and is of dimension $N \times F$. Each column has N elements corresponding to measurements of all spectrum sensors. In other words, each column of \mathbf{Y}^t is a 1D collection of all power spectrum sensors within the 2D network. The order for vectorization is arbitrary; however, in Line 9, the

operator reshape is the inverse operator for the employed vectorization. Here, Φ refers to the full spatial factors and A^t refers to the incomplete spatial maps corresponding to time slot t. CP decomposition using ALS can be categorized as a block coordinate descent algorithm. It is shown that if optimization along any coordinate direction yields a unique minimum point then the main cost function is convergent using a coordinate descent method [30]. Lines 3, 4 and 7 of TRASC is identical to the conventional ALS algorithm for CP decomposition. The main variables are computed in these three steps. However, we define a dependent variable which is obtained by interpolation of the spatial factors. Note that convergence of TRASC is inherited from convergence of ALS for CP decomposition [31].

IV. EXPERIMENTS

The TRASC algorithm is evaluated for dynamic spectrum cartography. The experimental setup is similar to that of [32]. Specifically, we consider F=16 channels and our area of interest with the size of $50\times 50~m^2$ is discretized into 51 horizontal bins and 51 vertical bins, i.e., N=2601. The primary active users are considered static and T=100 time slots are employed. The spatial propagation pattern of each transmitter is synthesized using a path-loss model and the spatial correlated log-normal shadowing model [33]. The spectral activity pattern of each transmitter is assumed as summation of three sinc functions as explained in [32] as

$$b_r(f) = \sum_{i=1}^{3} q_i^r \operatorname{sinc}^2(\frac{(f - f_i^r)}{w_i^r}),$$
 (12)

where, q_i^r follows a uniform distribution between 0.5 and 2. Moreover, f_i^r and w_i^r are the central frequency and the width parameter of each function, respectively. The width parameter is drawn from a uniform distribution between 2 and 4.

The performance of different spectrum sensing algorithms are evaluated via the Cartography Error, which is defined as

$$e = \frac{\|\log(\mathbf{Y}) - \log(\hat{\mathbf{Y}})\|_F}{\|\log(\mathbf{Y})\|_F}.$$
 (13)

Y indicates the power spectrum map and \hat{Y} refers to the interpolated map using a set of measurements. Employing logarithm scale results in less bias for high power spectrum areas of the network. Thus, we have a more reliable measure for comparison of the interpolated low-power details in the area of interest. Two different sensing patterns are employed as suggested in [32]. In the first pattern, a line of horizontal grid points and a line of vertical grid points are scanned. This pattern is referred as the structured pattern. The second pattern corresponds to random sampling of grid points in the network.

Fig. 2 shows the original power spectrum map in a frequency band which is sampled in a small subset of locations versus the recovered power spectrum map using different recovery algorithms. In Fig. 2b, the recovered spectrum using a plain CP decomposition is shown, i.e., only a low-rank decomposition is employed to interpolate the incomplete sensing results. The same strategy can be repeated using any other tensor

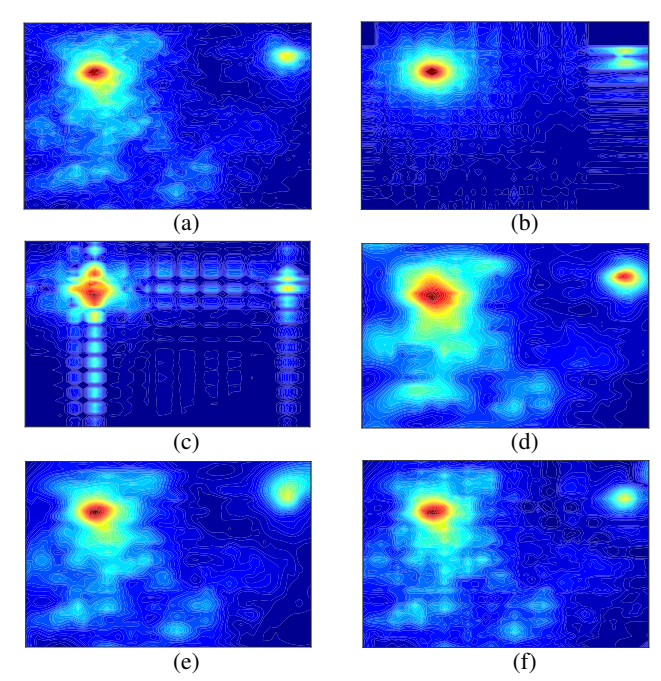


Fig. 2: Comparison between the original and the recovered spectrum maps. (a) The original power spectrum map. The grid is 50×50 , however, 6 columns and 6 rows of the original power spectrum map are measured. The power spectrum is measured at these locations only. (b) The recovered spectrum from missing and noisy sensed data using a plain CP decomposition and interpolating the unread measurements via CP reconstruction. (c) The recovered spectrum via block-term decomposition. (d) The plain 2D plate splines method is employed for interpolating the power spectrum map. (e) The proposed method in [32] via the block-term decomposition which post-processed using 2D plate splines. (f) Our proposed method that employs CP decomposition and 2D plate splines jointly.

decomposition model. Fig. 2c shows the interpolation result using the plain block-term tensor decomposition [32]. Kernelbased interpolation methods interpolate the incomplete set of measurements via neighborhood information. However, these methods neglect the global correlation among measurements in space, spectral bands and time. Fig. 2d shows the interpolated map using 2D plate splines method [34]. Fig. 2e shows the result of coupled BTD where the pathloss gains are corrected using plate splines as a post-processing. In Fig. 2f, our proposed framework is evaluated which employs an iterative approach between model-based CP factors and neighborhoodbased splines. The last two subfigures correspond to the joint methods that exploit both tensor-based decomposition and interpolation. Utilizing both techniques improves the accuracy of spectrum recovery. Our proposed joint method estimates the low-power source at the top right of the area more accurate.

Fig. 3 exhibits two interpolated CP spatial components. At each iteration of TRASC, a set of spatial CP factors are estimated and interpolated. Plate splines method is utilized to obtain interpolated CP factors as the basic components to reconstruct the desired spectrum map. In the next experiment, we study the performance of two basic methods based on tensor decomposition and neighborhood interpolation in terms of the normalized error of cartography defined in (13). Moreover, in this experiment we consider the BTD method for cartography [32]. Fig. 4b shows the cartography error of different methods over time. Tensor-based methods need a fine tuning of rank in practice. In this experiment it is assumed

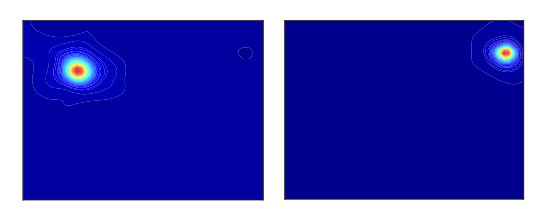


Fig. 3: The interpolated spatial components using our proposed framework. The rank of CPD is assumed to be 2. A linear combination of these two factors is able to reconstructs the power spectrum map in any frequency band.

that the assumed rank differs +1 from the best possible rank. As it can be seen and as it is mentioned in [32], the block-term tensor decomposition is highly sensitive to the rank. However, our proposed structured CP decomposition is not highly sensitive to the rank. In Fig.4b the cartography error for 100 time slots is plotted. Tensor-based methods also are compared with the naive interpolation on independent channels for each time slot using TPS interpolation. In some time slots, the performance of the coupled block-term decomposition is close to the performance of our framework. However, the coupled block-term decomposition is performing worse than TRASC in average over time.

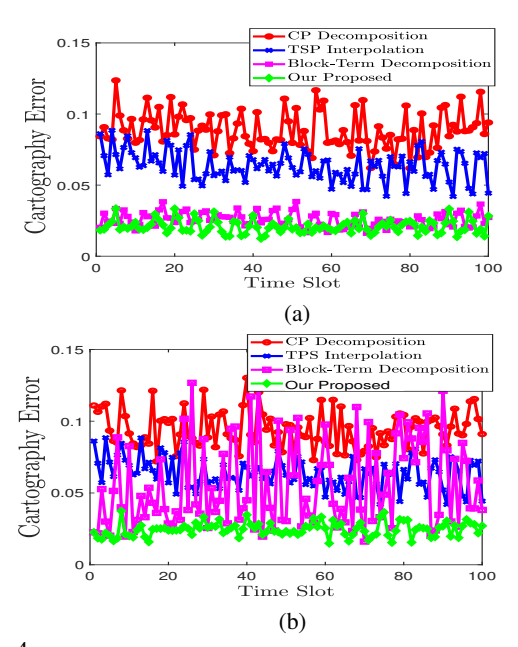


Fig. 4: Spectrum map reconstruction error for several algorithms. (a) The rank for the tensor-based methods is assumed to be the best possible rank. (b) The rank for the tensor-based methods is assumed to differ from the best possible rank by +1.

Unlike the coupled block-term decomposition method [32], our framework is an iterative approach which performs both tensor decomposition and 2D spline interpolation at each iteration. However, any iterative approach raises the convergence issue which must be investigated. Fig. 5 shows the performance of the proposed framework over iterations in terms of the normalized cartography error.

An adaptive rank estimation method introduced in the previous section is presented next. Fig. 6 shows the residual error of the main cost function (10) versus the assumed rank. There are two static sources in the area and each one has

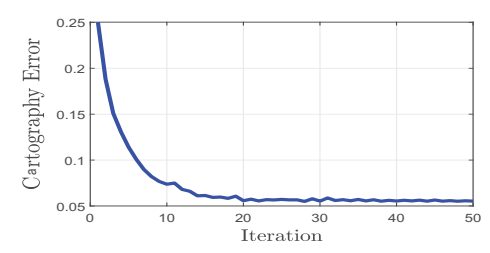


Fig. 5: The convergence behavior of the proposed framework. At each iteration, all tensor CP factors are updated and a more accurate model is estimated for reconstruction of power spectrum map.

three active bands based on (12). The cartography error can be interpreted as a generalized error for unseen grid points and the residual error represents the error of TRASC only for the sensed grid points. This concept is similar to the train error and the test error in machine learning systems. Increasing the rank improves the residual error, however, after a certain point it will cause over-fitting for the general cartography error.

The behavior of TRASC w.r.t. the assumed rank is smooth while the method based on BTD introduced in [32] is highly sensitive to the assumed rank of BTD. Fig. 7 shows the sensitivity of cartography based on BTD w.r.t. the assumed rank. As it can be seen, this method only performs efficiently for a specific rank. This problem makes BTD not viable in the cartography application.

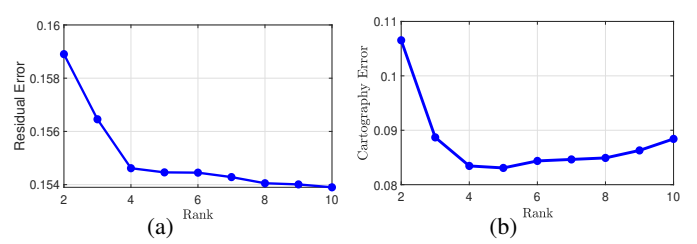


Fig. 6: (a) The effect of assumed rank on the residual error of cost function (10). (b) Sensitivity to the proposed framework w.r.t. the assumed CP rank.

In Fig. 8a, our proposed spectrum sensing framework is compared with the block-term tensor decomposition in terms of the number of sensed grid points. In structured sampling an entire line of horizontal/vertical grid points are sensed. However, in the random sampling the sensed grid points have no spatial structure.

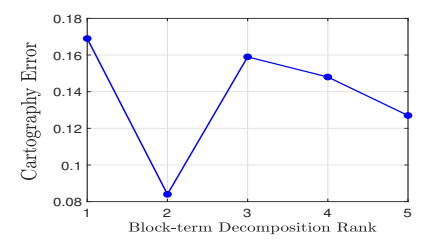


Fig. 7: Sensitivity of BTD to the assumed rank.

At each iteration of our framework, a 2D interpolation is applied on all spatial CP factors. The impact of the regularization parameter which controls the smoothness of interpolation functions is studied in Fig. 9. A low value for parameter α corresponds to a non-smooth interpolating function. However, there is a wide range for the smoothing parameter such that the cartography error is improved.

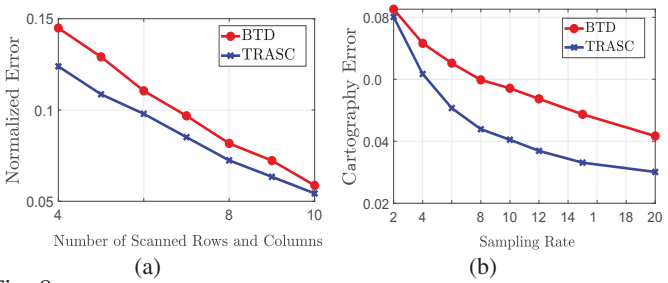


Fig. 8: (a) The number of structured measurements versus the normalized cartography error. (b) The number of random measurements versus the normalized cartography error.

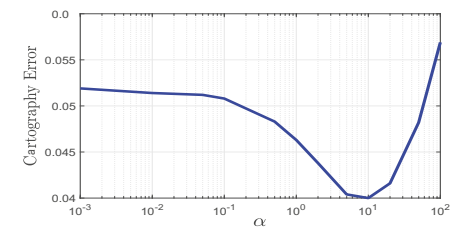


Fig. 9: The impact of the smoothness parameter in 2D splines interpolation on the overall performance of the proposed framework.

V. CONCLUSION

A new framework for dynamic spectrum cartography is proposed. The thin plate spline interpolation method and the tensor CP decomposition algorithm are employed jointly in a unified framework. An iterative algorithm, referred to as TRASC, is introduced for estimating CP factors and the parameters of interpolation. The proposed joint decomposition and interpolation is used for tensor completion to address the problem of spectrum cartography under the shadowing channel model. Our proposed cartography technique is shown to be as accurate as the state-of-the-art method while it is less sensitive to the model's parameters such as the assumed rank of tensors.

REFERENCES

- O. H. Toma, M. López-Benítez, D. K. Patel, and K. Umebayashi, "Estimation of primary channel activity statistics in cognitive radio based on imperfect spectrum sensing," *IEEE Trans. on Communications*, 2020.
- [2] W. Zhang, C.-X. Wang, X. Ge, and Y. Chen, "Enhanced 5g cognitive radio networks based on spectrum sharing and spectrum aggregation," *IEEE Trans. on Communications*, vol. 66, no. 12, pp. 6304–6316, 2018.
- [3] W. Ahmad, N. Radzi, F. Samidi, A. Ismail, F. Abdullah, M. Jamaludin, and M. Zakaria, "5G technology: Towards dynamic spectrum sharing using cognitive radio networks," *IEEE Access*, vol. 8, 2020.
- [4] I. F. Akyildiz, W.-Y. Lee, M. C. Vuran, and S. Mohanty, "Next generation/dynamic spectrum access/cognitive radio wireless networks: A survey," *Computer Networks*, vol. 50, no. 13, pp. 2127 – 2159, 2006.
- [5] S. Haykin, "Cognitive radio: brain-empowered wireless communications," *IEEE Journal on Selected Areas in Communications*, vol. 23, no. 2, pp. 201–220, Feb. 2005.
- [6] A. Zaeemzadeh, M. Joneidi, N. Rahnavard, and G. Qi, "Co-spot: Cooperative spectrum opportunity detection using bayesian clustering in spectrum-heterogeneous cognitive radio networks," *IEEE Trans. on Cognitive Communications and Networking*, vol. 4, pp. 206–219, 2018.
- [7] N. Muchandi and R. Khanai, "Cognitive radio spectrum sensing: A survey," in 2016 International Conference on Electrical, Electronics, and Optimization Techniques (ICEEOT). IEEE, 2016, pp. 3233–3237.
- [8] Y. Chen, S. Su, H. Yin, X. Guo, Z. Zuo, J. Wei, and L. Zhang, "Optimized non-cooperative spectrum sensing algorithm in cognitive wireless sensor networks," *Sensors*, 2019.
- [9] B. Hamdaoui, B. Khalfi, and M. Guizani, "Compressed wideband spectrum sensing: Concept, challenges, and enablers," *IEEE Communications Magazine*, 2018.

- [10] S. Kapoor and G. Singh, "Non-cooperative spectrum sensing: A hybrid model approach," in 2011 International Conference on Devices and Communications (ICDeCom), Feb 2011, pp. 1–5.
- [11] J. Bazerque and G. Giannakis, "Distributed spectrum sensing for cognitive radio networks by exploiting sparsity," *IEEE Trans. on Signal Processing*, vol. 58, no. 3, pp. 1847–1862, March 2010.
- [12] D. Cohen, A. Akiva, B. Avraham, and Y. C. Eldar, "Centralized cooperative spectrum sensing from sub-nyquist samples for cognitive radios," in *IEEE Inter. Conference on Communications (ICC)*, 2015, pp. 7486–7491.
- [13] J. Wei and X. Zhang, "Energy-efficient distributed spectrum sensing for wireless cognitive radio networks," in 2010 INFOCOM IEEE Conference on Computer Communications Workshops. IEEE, 2010, pp. 1–6.
- [14] M. Joneidi, H. Yazdani, A. Vosoughi, and N. Rahnavard, "Source localization and tracking for dynamic radio cartography using directional antennas," in *IEEE International Conference on Sensing, Communica*tion, and Networking (SECON), 2019, pp. 1–9.
- [15] H. Yazdani and A. Vosoughi, "On cognitive radio systems with directional antennas and imperfect spectrum sensing," in 2017 IEEE International Conference on Acoustics, Speech and Signal Processing (ICASSP). IEEE, 2017, pp. 3589–3593.
- [16] Y. Luo, J. Dang, and Z. Song, "Optimal compressive spectrum sensing based on sparsity order estimation in wideband cognitive radios," *IEEE Trans. on Vehicular Technology*, pp. 1–1, 2019.
- [17] E. Dall'Anese, J. A. Bazerque, and G. B. Giannakis, "Group sparse lasso for cognitive network sensing robust to model uncertainties and outliers," *Physical Communication*, vol. 5, no. 2, pp. 161 – 172, 2012, compressive Sensing in Communications.
- [18] X. Fu, N. D. Sidiropoulos, and W.-K. Ma, "Power spectra separation via structured matrix factorization." *IEEE Trans. Signal Processing*, vol. 64, no. 17, pp. 4592–4605, 2016.
- [19] J. D. Carroll and J.-J. Chang, "Analysis of individual differences in multidimensional scaling via an n-way generalization of "eckart-young" decomposition," *Psychometrika*, vol. 35, no. 3, pp. 283–319, 1970.
- [20] L. R. Tucker, "Some mathematical notes on three-mode factor analysis," *Psychometrika*, vol. 31, no. 3, pp. 279–311, 1966.
- [21] T. G. Kolda and B. W. Bader, "Tensor decompositions and applications," SIAM review, vol. 51, no. 3, pp. 455–500, 2009.
- [22] P. Comon, "Tensors: a brief introduction," IEEE Signal Processing Magazine, vol. 31, no. 3, pp. 44–53, 2014.
- [23] B. Recht, M. Fazel, and P. A. Parrilo, "Guaranteed minimum-rank solutions of linear matrix equations via nuclear norm minimization," SIAM review, vol. 52, no. 3, pp. 471–501, 2010.
- [24] S. Friedland and L.-H. Lim, "Nuclear norm of higher-order tensors," Mathematics of Computation, vol. 87, no. 311, pp. 1255–1281, 2018.
- [25] P. Comon, X. Luciani, and A. L. De Almeida, "Tensor decompositions, alternating least squares and other tales," *Journal of Chemometrics*, vol. 23, no. 7-8, pp. 393–405, 2009.
- [26] J. A. Bazerque, G. Mateos, and G. B. Giannakis, "Group-lasso on splines for spectrum cartography," *IEEE Trans. on Signal Processing*, vol. 59, no. 10, pp. 4648–4663, 2011.
- 27] G. Wahba, Spline models for observational data. SIAM, 1990.
- [28] M. Joneidi, A. Zaeemzadeh, and N. Rahnavard, "Dynamic sensor selection for reliable spectrum sensing via e-optimal criterion," in 2017 IEEE International Conf. on Mobile Ad Hoc and Sensor Systems (MASS).
- [29] M. Joneidi, A. Zaeemzadeh, B. Shahrasbi, G. Qi, and N. Rahnavard, "E-optimal sensor selection for compressive sensing-based purposes," *IEEE Trans. on Big Data*, pp. 1–1, 2018.
- [30] D. G. Luenberger, Optimization by vector space methods. John Wiley & Sons, 1997.
- [31] A. Uschmajew, "Local convergence of the alternating least squares algorithm for canonical tensor approximation," SIAM Journal on Matrix Analysis and Applications, vol. 33, no. 2, pp. 639–652, 2012.
- [32] G. Zhang, X. Fu, J. Wang, X.-L. Zhao, and M. Hong, "Spectrum cartography via coupled block-term tensor decomposition," *IEEE Trans.* on Signal Processing, 2020.
- [33] A. Goldsmith, *Wireless communications*. Cambridge university press, 2005.
- [34] D. Romero, S.-J. Kim, G. B. Giannakis, and R. López-Valcarce, "Learning power spectrum maps from quantized power measurements," *IEEE Trans. on Signal Processing*, vol. 65, no. 10, pp. 2547–2560, 2017.